

Advanced Analytical Approaches for Nonlinear Fractional PDEs Reduced Differential Transform Method and Elzaki Transform Homotopy Perturbation Method

Zahid Ullah¹, Jianghao Hao¹, Ali Akgül^{2,3,4,5,6}, Thabet Abdeljawad^{7,8,9,10,*}, Manar A. Alqudah¹¹, Ihtisham Ul Haq¹²

School of Mathematics and Statistics, Shanxi University, Taiyuan, China

²*Department of Electronics and Communication Engineering, Saveetha School of Engineering, SIMATS, Chennai, Tamilnadu, India.*

³*Siirt University, Art and Science Faculty, Department of Mathematics, 56100 Siirt, Turkey.*

⁴*Department of Computer Engineering, Biruni University, 34010 Topkapı, Istanbul, Turkey.*

⁵*Near East University, Mathematics Research Center, Department of Mathematics, Near East Boulevard, PC: 99138, Nicosia /Mersin 10 – Turkey.*

⁶*Applied Science Research Center. Applied Science Private University, Amman, Jordan.*

⁷*Department of Mathematics and Sciences, Prince Sultan University, P.O. Box 66833, 11586 Riyadh, Saudi Arabia*

⁸*Center for Applied Mathematics and Bioinformatics (CAMB), Gulf University for Science and Technology, Hawally, 32093, Kuwait*

⁹*Department of Medical Research, China Medical University, Taichung 40402, Taiwan*

¹⁰*Department of Mathematics and Applied Mathematics, Sefako Makgatho Health Sciences University, Garankuwa, Medusa 0204, South Africa*

¹¹*Department of Mathematical Sciences, College of Sciences, Princess Nourah bint Abdulrahman University, P. O. Box 84428 Riyadh 11671, Saudi Arabia*

¹²*School of Mathematics, Nagoya University, Furo-cho, Chikusa-ku, Nagoya, 464-8602, Japan*

Received April 2025 Accepted May 2025 Published June 2025

Abstract

This study presents a comparative analysis of two advanced analytical methods—the Elzaki Transform Homotopy Perturbation Method (ETHPM) and the Fractional Reduced Differential Transform Method (FRDTM)—for solving nonlinear fractional partial differential equations (FPDEs) arising in biological population dynamics. After establishing the mathematical foundations of fractional calculus, the Elzaki transform, and homotopy perturbation theory, we demonstrate the applicability of both methods to FPDEs modeling population growth and swarm behavior. Our results reveal that ETHPM and FRDTM yield highly accurate approxi-

Email address: zahidmath1233@gmail.com, hjhao@sxu.edu.cn, aliakgul00727@gmail.com, tabdeljawad@psu.edu.sa, maalqudah@pnu.edu.sa, ihtisham.ul.haq.d2@math.nagoya-u.ac.jp (Zahid Ullah¹, Jianghao Hao¹, Ali Akgül^{2,3,4,5,6}, Thabet Abdeljawad^{7,8,9,10,*}, Manar A. Alqudah¹¹, Ihtisham Ul Haq¹²)

mate solutions, underscoring their efficacy as computational tools for complex biological systems. The study highlights the broader implications of these fractional-order models in ecology and population dynamics, bridging theoretical mathematics with practical applications in life sciences. Through systematic comparisons, we provide insights into the strengths and limitations of each method, offering valuable guidance for researchers working with nonlinear fractional systems in biological contexts.

Keywords: Fractional-type derivatives, Elzaki transform homotopy perturbation method, fractional reduced differential transform method, Riemann–Liouville fractional integral

1. Introduction

Fractional calculus has gained significant attention in recent years because of its ability to describe complex phenomena in various scientific and engineering disciplines more accurately than classical integer-order calculus. In the realm of biological population dynamics, fractional-order models offer a more realistic approach to capture the memory and hereditary characteristics of populations, which are often overlooked in classical models [1]. The Elzaki transform method has emerged in the past decade as one of the potential tools of mathematics to solve fractional-order differential equations [2]. Due to the simplicity and efficiency in the conversion of fractional differential equations into (ODEs) [4], this method has been applied to various problems in science and engineering [5]. In this work, we will present a two-dimensional fractional order time model of biological population by means of the Elzaki transform technique [6]. The model is designed to capture the intricate dynamics of biological populations by incorporating fractional-order derivatives to account for memory and hereditary effects [7]. We aim to derive an analytical solution to this model using the Elzaki transform method [8], providing a comprehensive understanding of the temporal and spatial evolution of the biological population under consideration. The analytical solution obtained will serve as a valuable tool for predicting and analyzing the behavior of biological populations, which can have significant implications in ecology, epidemiology, and conservation biology [9]. Furthermore, the proposed model and solution will be validated through numerical simulations and comparisons with existing models to demonstrate their effectiveness and accuracy [10].

It is normally argued by the biological scientists that emigration [11], otherwise known as dispersal [12], forms a critical determinant of the species populations [13]. The spatial distribution of a species is described by three primary functions $\vec{x} = (x, l)$ within a given region D where $l \geq 0$. These functions detail the diffusion velocity, $u(\vec{x}, l)$ the population density $q(\vec{x}, l)$ and supply $g(\vec{x}, l)$. Specifically, $q(\vec{x}, l)$ indicates

the rate of change in population due to births and deaths per unit volume, while $\dot{v}(\vec{x}, l)$ is a number denoting the number of individuals. Moreover, $\dot{u}(\vec{x}, l)$ provides the mean velocity of people describing the flux of the population from one place to another [14]. For any $C \subseteq E$ sub-region, the functions \dot{q} , \dot{v} , and \dot{g} should agree with each other [15].

$$\frac{d^\mu}{dV^\mu} \int_C \dot{q} dU + \int_{\partial C} \dot{q} \dot{v} \cdot \hat{n} dA = \int_C \dot{g} dU, \tag{1}$$

Here \hat{n} represents the unit normal vector pointing outward from the boundary ∂C of C [16]. This principle asserts that the rate of change of the population within C combined with the rate at which animals exit C through its boundary, equals the rate at which animals enter C [17]. Gurtin and Maccamy [18] demonstrated this by imposing certain conditions. Assume the result to be as follows:

$$\dot{g} = \dot{g}(\dot{q}), \quad \dot{v} = -k(\dot{q})\nabla\dot{q}. \tag{2}$$

If $k(\dot{q}) > 0$ when $\dot{q} > 0$ and ∇ denotes the Laplace operator, then the resulting equations for the density of \dot{q} are given by the following two-dimensional nonlinear degenerate parabolic PDEs.

$$\dot{q}_l^\alpha = \phi(\dot{q})_{xx} + \phi(\dot{q})_{yy} + \dot{g}(\dot{q}), \quad l \geq 0, \quad \dot{x}, \dot{y} \in \mathbb{C}. \tag{3}$$

Gurney et al. [17] applied a particular instance of $\phi(\dot{q})$ to simulate animal population dynamics [19]. Population movement [20] is influenced by either adult individuals being displaced by newcomers or by younger individuals [21] departing from their birthplaces to create their own [22] reproductive territories. In both scenarios, it is assumed that the movement [23] occurs to a nearby unoccupied area. In the presented model, movement predominantly occurs along the population density gradient, making the model more suitable for high-density population areas than low-density ones. They analyzed a rectangular region where an animal could either stay in its current location or migrate from an area of high density to one of lower density. In these scenarios, the probability distribution is determined by the gradient magnitude of the population density at each grid point [24].

This model then yields equation (1). If $\phi(\dot{q}) = \dot{q}^2$, the equation becomes:

$$\dot{q}_l^\alpha = \dot{q}_{xx}^2 + \dot{q}_{yy}^2 + \dot{g}(\dot{q}), \quad l \geq 0, \quad \dot{x}, \dot{y} \in \mathbb{C} \tag{4}$$

Given the initial condition $\dot{q}(\dot{x}, \dot{y}, 0)$, examined several characteristics of equation (4), including Hölder estimates of its solutions, by Y.G. Lu [18]. Two constitutive models for \dot{g} can be based on the Malthusian law:

$$\dot{g}(\dot{q}) = \mu \dot{q}, \quad (\mu = \text{constant}) \tag{5}$$

and the Verhulst law:

$$\dot{g}(\dot{q}) = \mu_1 \dot{q} - \mu_2 \dot{q}^2. \tag{6}$$

where μ_1 and μ_2 are positive constants, which represents the Verhulst Law [12]. We extend \dot{g} to a more generalized form defined as:

$$\dot{g}(\dot{q}) = h \dot{q}^\alpha (1 - r \dot{q}^\beta) \tag{7}$$

which yields

$$\dot{q}_l^\alpha = \dot{q}_{xx}^2 + \dot{q}_{yy}^2 + h \dot{q}^\alpha (1 - r \dot{q}^\beta), \quad l \geq 0, \quad \dot{x}, \dot{y} \in \mathbb{C} \tag{8}$$

where $\alpha, \beta, h,$ and r are real-valued constants. It is important to note that the Malthusian law and the Verhulst law are specific cases derived when certain conditions are applied:

1. Malthusian law: $h = \mu, \alpha = 1, r = 0$
2. Verhulst law: $h = \mu, \alpha = \beta = 1, r = \frac{\gamma}{\mu}$

2. Preliminaries

Definition 2.1. A real function $g(l), l > 0,$ is considered to belong to the space $D_\alpha, \alpha \in \mathbb{R}$ if \exists a real number $(q > \alpha)$ s.t $g(l) = l^q g_1(l),$ where $g_1 \in D[0, \infty].$ It is evident that, $D_\alpha \subset D_\beta$ if $\beta \leq \alpha$ [19].

Definition 2.2. A function $g(l), l > 0,$ is considered to be in the space $D_a^m, m \in \mathbb{N} \cup \{0\},$ if $g^{(m)} \in D_\alpha$ [19]. In this context, we will introduce some fundamental concepts of fractional calculus and natural transforms.

Definition 2.3. The left-sided Riemann-Liouville fractional integral of a is greater then zero function is given by the following expression [15]:

$$\begin{cases} J^a f(x) = \frac{1}{\Gamma(a)} \int_0^x (x-t)^{a-1} f(t) dt, & a > 0, x > 0 \\ J^0 f(x) = f(x), & x = 0 \end{cases} \tag{9}$$

The application of the Riemann-Liouville fractional derivative approach to model the real-world phenomena described by fractional differential equations suffers from certain disadvantages. Caputo and Mainardi

[16] have, in their investigation within the theory of viscoelasticity, introduced a modified fractional differentiation operator C to extend the abilities of the Riemann-Liouville fractional derivative in modeling real applications.

Definition 2.4. *The Caputo definition of the fractional derivative of order m of function $f(t)$ is described by [17]:*

$$G^a T^a f(x) = T^{m-a} G^m f(x) = \frac{1}{\Gamma(m-a)} \int_0^x (x-t)^{m-a-1} f^{(m)}(t) dt, \tag{10}$$

for $m - 1 < a < m$, $m \in \mathbb{N}$, and $f \in C^m$, $a > 0$, $x > 0$.

Lemma 2.1. *If $m - 1 < a \leq m$, $m \in \mathbb{N}$, and $f \in C^m_\mu$, $\mu \geq -1$, then*

$$\begin{cases} G^a T^a f = f(x), & x > 0 \\ T^a G^a f = f(x) - \sum_{k=0}^m f^{(k)}(0^+) \frac{x^k}{k!}, & x > 0 \end{cases} \tag{11}$$

The present work, the Caputo FD has been chosen for its flexibility in accommodating standard initial and boundary conditions while formulating problems of physical. Other important properties of the fractional derivatives are given in [17, 18].

3. Elzaki Transform Homotopy Perturbation Method (ETHPM)

Here one will learn how the ETHPM algorithm is used to solve both types of fractional partial differential equations: those that are linear and nonlinear.

$$G_\delta^\eta \dot{u}(\mu, \delta) + T \dot{u}(\mu, \delta) + \mathbb{N} \dot{u}(\mu, \delta) = \Phi(\mu, \delta), \quad \mu \geq 0, \quad r - 1 < \eta \leq r \tag{12}$$

where $G_\delta^\eta = \frac{\partial^\eta}{\partial \delta^\eta}$ denotes the order η fractional derivative, T is a linear operator, F is a Non-linear function, and the source function is Φ .

$$\begin{cases} u(\mu, 0) = \Phi(\mu), & 0 < \eta \leq 1, \\ u(\mu, 0) = \Phi(\mu), \\ \frac{\partial u(\mu, 0)}{\partial \delta} = \Phi(\mu), & 1 < \eta \leq 2. \end{cases} \tag{13}$$

Applying the linearity of ETHP to both equations (13) one gets

$$\dot{E}[G_\delta^\eta u(\mu, \delta)] + \dot{E}[Tu(\mu, \delta)] + \dot{E}[Nu(\mu, \delta)] = \dot{E}[N(\mu, \delta)], \quad \eta > 0 \tag{14}$$

Using the property of ETHP, we get

$$\left\{ \frac{\partial u(\mu, \delta)}{\partial \beta^\eta} - C + \dot{E}[Tu(\mu, \delta)] + \dot{E}[Nu(\mu, \delta)] = \dot{E}[N(\mu, \delta)] \quad \eta > 0 \right. \tag{15}$$

where

$$C = \sum_k^{n-1} \beta^{2-\eta+\kappa} u^\kappa(\mu, 0),$$

$$u(\mu, \beta) = \beta^\eta \dot{E}[N(\mu, \delta)] + \beta^\eta C - \beta^\eta \dot{E}[Tu(\mu, \delta)] - \beta^\eta \dot{E}[Nu(\mu, \delta)] \tag{16}$$

Taking the inverse ETHP to both equations (17), we get

$$u(\mu, \delta) = S(\mu, \delta) - E^{-1}[\beta^\eta E[Tu(\mu, \delta) + Nu(\mu, \delta)]] \tag{17}$$

The HPM approach is now applied, where $S(\mu, \delta)$ represents the term derived from the initial conditions

$$u(\mu, \delta) = \sum_{k=0}^{\infty} Q^k u_k(\mu, \delta) \tag{18}$$

The nonlinear operator can be expressed in the following decomposed form:

$$Mu(\mu, \delta) = \sum_{k=0}^{\infty} Q^k I_n(u) \tag{19}$$

Where $I_n(u)$ are given by

$$I_n(u_1, u_2, u_3, \dots, u_n) = \frac{1}{n!} \frac{\partial}{\partial Q^n} \left[M \left(\sum_{i=0}^{\infty} Q^i u_i \right) \right]_{L=0}, \quad n = 1, 2, \dots \tag{20}$$

When we substitute equations (20) and (19) into equation (18), we get

$$\sum_n^{\infty} Q^n u_n(\mu, \delta) = H(\mu, \delta) - QF^{-1}[\beta^\eta E[T \sum_{i=0}^{\infty} u_n(\mu, \delta) + M \sum_{n=0}^{\infty} Q^n I(u_n)]] \tag{21}$$

This is the combination of ETM and HPM by using He’s polynomials. Equating coefficients, we get the following:

$$\begin{aligned}
 Q_0 : u_0(\mu, \delta) &= I(\mu, \delta), \\
 Q_1 : u_1(\mu, \delta) &= -F^{-1}[C^\eta E[S u_0(\mu, \delta) + I_0(\mu, \delta)], \\
 Q_2 : u_2(\mu, \delta) &= -E^{-1}[C^\eta E[S u_1(\mu, \delta) + I_1(u)]], \\
 Q_3 : u_3(\mu, \delta) &= -E^{-1}[C^\eta E[S u_2(\mu, \delta) + I_2(u)]], \\
 &\cdot \\
 &\cdot \\
 &\cdot
 \end{aligned}$$

Then the solution is

$$u(\mu, \delta) = \lim_{p \rightarrow 1} u_n(\mu, \delta) = u_0(\mu, \delta) + u_1(\mu, \delta) + u_2(\mu, \delta) + \dots,$$

4. Fractional reduced differential transform method (FRDTM)

This context, presents basic definitions and important properties of the fractional reduced differential transform method. Assume that $W(y, \ell)$ can be written as a product of two functions of a one variable, that is $W(y, \ell) = G(y)H(\ell)$. The function $W(y, \ell)$ can be represented in the form using properties of 1 D differential transforms:

$$W(y, \ell) = \sum_{j=0}^{\infty} G(j) y^j \sum_{i=0}^{\infty} H(i) \ell^i = \sum_{j=0}^{\infty} \sum_{i=0}^{\infty} W(j, i) y^j \ell^i \tag{22}$$

Here $W(j, i) = G(j)H(i)$ is says that the spectrum of the function $W(y, \ell)$. Suppose \mathbb{R}_D represent the mathematical operator that is used to compute the RDT and \mathbb{R}_D^{-1} represent the inverse operation that reverses the transform process [4].

Definition 4.1. *Provided that the function $W(y, \ell)$ is mathematically expressed with derivatives and is smooth about the spatial variable y and time variable ℓ in the domain of interest, then the spectrum function, which represents how the function varies across time (ℓ -dimensions),*

$$W_{\mathbb{k}}(y) = \frac{1}{\Gamma(\mathbb{k}\alpha + 1)} \left[\frac{\partial^{\mathbb{k}}}{\partial \ell^{\mathbb{k}}} W(y, \ell) \right]_{\ell=\ell_0} \tag{23}$$

is a function derived from $W(y, \ell)$ through fractional transformation, where α is an adjustable parameter that characterizes the fractional derivative's temporal order. In this paper, the lowercase notation $W(y, \ell)$ will refer to the initial function whereas the uppercase notation refers to its fractional reduced transformed form as $W_{\mathbb{k}}(y)$ and mathematically defined as:

$$W(y, \ell) = \sum_{\mathbb{k}=0}^{\infty} W_{\mathbb{k}} (\ell - \ell_0)^{\mathbb{k}\alpha}. \tag{24}$$

From Eqs. (23) and (24), we get

$$W(y, \ell) = \sum_{\mathbb{k}=0}^{\infty} \frac{1}{\Gamma(\mathbb{k}\alpha + 1)} \left[\frac{\partial^{\mathbb{k}}}{\partial \ell^{\mathbb{k}}} W(y, \ell) \right]_{\ell=\ell_0} (\ell - \ell_0)^{\mathbb{k}\alpha}. \tag{25}$$

If $\ell = 0$, Eq. (25) becomes

$$W(y, \ell) = \sum_{\mathbb{k}=0}^{\infty} \frac{1}{\Gamma(\mathbb{k}\alpha + 1)} \left[\frac{\partial^{\mathbb{k}}}{\partial \ell^{\mathbb{k}}} W(y, \ell) \right]_{\ell=0} (\ell)^{\mathbb{k}\alpha}. \tag{26}$$

A fundamental principle of the FRDT method is that the power series expansion represents any given function. This indicates that the FRDT for a function is found from the FD of a developed power expansion for a given function.

Definition 4.2. If $v = (y, \ell) = \mathbb{R}_D^{-1} [V_{\mathbb{k}}(y)]$, $u(y, \ell) = \mathbb{R}_D^{-1} [U_{\mathbb{k}}(y)]$ and the convolution \otimes representing multiplication in the context of the (FRDT), then the fundamental operations of FRDT are defined. Here Γ denotes the Gamma function, a well-known mathematical function:

$$\Gamma(T) := \int_0^{\infty} e^{-\ell} \ell^{T-1} \partial \ell, T \in D \tag{27}$$

The Gamma function in this case is a continuous equivalent of the factorial function [3]. It can be applied to any positive real number; Unlike the factorial function, it is defined only for non-negative integers. The Gamma function, denoted by $\Gamma(T)$, is a mathematical function that extends the concept of the factorial function to non-integer values. The gamma function satisfies the recurrence relation of $\Gamma(T + 1) = T\Gamma(T)$ for all $T > 0$.

5. Examples

Example 1. The biological population model of fractional-order is described as follows:

$$\frac{\partial^\alpha S}{\partial t^\alpha} = \frac{\partial^2 S^2}{\partial x^2} + \frac{\partial^2 S^2}{\partial y^2} + \eta S. \tag{28}$$

The condition at the start is

$$S_0(\dot{x}, \dot{y}, 0) = \sqrt{\dot{x}\dot{y}}. \tag{29}$$

Substituting the FRDTM into both of aspect (29) and subject to equation (28), we have

$$\frac{\Gamma(k\alpha + \alpha + 1)}{\Gamma(k\alpha + 1)} S_{k+1}(\dot{x}, \dot{y}) = \frac{\partial^2}{\partial \dot{x}^2} \left[\sum_{r=0}^{\infty} S_r(\dot{x}, \dot{y}) S_{k-1}(\dot{x}, \dot{y}) \right] + \frac{\partial^2}{\partial \dot{y}^2} \left[\sum_{r=0}^{\infty} S_r(\dot{x}, \dot{y}) S_{k-1}(\dot{x}, \dot{y}) \right] + \eta [S_k(\dot{x}, \dot{y})]. \tag{30}$$

For the case of the **FRDTM** initial condition we find:

$$S_0(\dot{x}, \dot{y}) = \sqrt{\dot{x}\dot{y}}. \tag{31}$$

putting Eq. (31) in Eq. (30) we get $S_k(\dot{x}, \dot{y})$, $k = 1, 2, 3, \dots$:

$$\begin{aligned} S_1(\dot{x}, \dot{y}) &= \frac{\eta}{\Gamma(\alpha + 1)} \sqrt{\dot{x}\dot{y}}, \\ S_2(\dot{x}, \dot{y}) &= \frac{\eta^2}{\Gamma(2\alpha + 1)} \sqrt{\dot{x}\dot{y}}, \\ S_3(\dot{x}, \dot{y}) &= \frac{\eta^3}{\Gamma(3\alpha + 1)} \sqrt{\dot{x}\dot{y}}, \\ S_4(\dot{x}, \dot{y}) &= \frac{\eta^4}{\Gamma(4\alpha + 1)} \sqrt{\dot{x}\dot{y}}, \\ &\vdots \\ S_k(\dot{x}, \dot{y}) &= \frac{\eta^k}{\Gamma(k\alpha + 1)} \sqrt{\dot{x}\dot{y}}. \end{aligned}$$

It uses the inverse of the differential reduced transform of $S_k(\dot{x}, \dot{y})$, $k = 1, 2, 3, \dots$, we get

$$S(\dot{x}, \dot{y}, t) = \sum_{k=0}^{\infty} S_k(\dot{x}, \dot{y}) t^{\dot{k}\alpha} = S_0(\dot{x}, \dot{y}) + S_1(\dot{x}, \dot{y}) t^{\dot{\alpha}} + S_2(\dot{x}, \dot{y}) t^{2\dot{\alpha}} + S_3(\dot{x}, \dot{y}) t^{3\dot{\alpha}} + \dots \tag{32}$$

$$= \sqrt{\dot{x}\dot{y}} \left(1 + \frac{\eta}{\Gamma(\dot{\alpha} + 1)} t^{\dot{\alpha}} + \frac{\eta^2}{\Gamma(2\dot{\alpha} + 1)} t^{2\dot{\alpha}} + \frac{\eta^3}{\Gamma(3\dot{\alpha} + 1)} t^{3\dot{\alpha}} + \dots \right) \tag{33}$$

$$= \sqrt{\dot{x}\dot{y}} \left[\sum_{k=0}^{\infty} \frac{(\eta t^\alpha)^k}{\Gamma(k\alpha + 1)} \right] \tag{34}$$

An exact solution is expressible as

$$S(\dot{x}, \dot{y}, t) = \sqrt{\dot{x}\dot{y}} F_\alpha(\eta t^\alpha). \tag{35}$$

The Mittag-Leffler function is given by $F_\alpha(\eta t) = \sum_{k=0}^{\infty} \frac{z^k}{\Gamma(k\alpha+1)}$. Where α is a parameter that generalizes the exponential function $\alpha \rightarrow 1$. The solution to this problem was earlier derived by Y. Liu et al. [13] and Arafa et al. [14] employing the Homotopy Analysis Method (HAM). HAM is a method used to approximate analytical solutions for nonlinear problems. When the parameter α approaches 1 in Equation (35), the expression simplifies to a different form:

$$S(\dot{x}, \dot{y}, t) = \sqrt{\dot{x}\dot{y}} \sum_{k=0}^{\infty} \frac{(\eta t)^k}{\Gamma(k+1)} = (\sqrt{\dot{x}\dot{y}}) e^{\eta t}. \tag{36}$$

Example 2. *he biological population model of fractional-order is described as follows:*

$$\frac{\partial^\alpha S}{\partial t^\alpha} = \frac{\partial^2 S^2}{\partial x^2} + \frac{\partial^2 S^2}{\partial y^2} + S, \tag{37}$$

The condition at the start is

$$S(\dot{x}, \dot{y}, 0) = \sqrt{\sin \dot{x} \sinh \dot{y}}. \tag{38}$$

For the case of the ****FRDTM**** initial condition we find:

$$\frac{\Gamma(k\alpha + \alpha + 1)}{\Gamma(k\alpha + 1)} S_{k+1}(\dot{x}, \dot{y}) = \frac{\partial^2}{\partial \dot{x}^2} \left[\sum_{r=0}^{\infty} S_r(\dot{x}, \dot{y}) S_{k-1}(\dot{x}, \dot{y}) \right] + \frac{\partial^2}{\partial \dot{y}^2} \left[\sum_{r=0}^{\infty} S_r(\dot{x}, \dot{y}) S_{k-1}(\dot{x}, \dot{y}) \right] + \eta [S_k(\dot{x}, \dot{y})]. \tag{39}$$

Application of this initial condition from the ****FRDTM**** gives

$$S_0(\dot{x}, \dot{y}, 0) = \sqrt{\sin \dot{x} \sinh \dot{y}} \tag{40}$$

Putting Eq. (41) in Eq. (40), for $S_k(\dot{x}, \dot{y})$ values:

$$\begin{aligned}
 S_1(\dot{x}, \dot{y}) &= \frac{1}{\Gamma(\alpha + 1)} \sqrt{\sin \dot{x} \sinh \dot{y}}, \\
 S_2(\dot{x}, \dot{y}) &= \frac{1}{\Gamma(2\alpha + 1)} \sqrt{\sin \dot{x} \sinh \dot{y}}, \\
 S_3(\dot{x}, \dot{y}) &= \frac{1}{\Gamma(3\alpha + 1)} \sqrt{\sin \dot{x} \sinh \dot{y}}, \\
 S_4(\dot{x}, \dot{y}) &= \frac{1}{\Gamma(4\alpha + 1)} \sqrt{\sin \dot{x} \sinh \dot{y}}, \\
 &\vdots \\
 S_k(\dot{x}, \dot{y}) &= \frac{1}{\Gamma(k\alpha + 1)} \sqrt{\sin \dot{x} \sinh \dot{y}}.
 \end{aligned}$$

It uses the inverse of the differential reduced transform of $S_k(\dot{x}, \dot{y})$, $k = 1, 2, 3, \dots$, we have

$$S(\dot{x}, \dot{y}, t) = \sum_{k=0}^{\infty} S_k(\dot{x}, \dot{y}) t^{k\alpha} = [S_0(\dot{x}, \dot{y}) + S_1(\dot{x}, \dot{y}) t^{\alpha} + S_2(\dot{x}, \dot{y}) t^{2\alpha} + S_3(\dot{x}, \dot{y}) t^{3\alpha} + \dots] \quad (41)$$

$$S(\dot{x}, \dot{y}, t) = \sqrt{\sin \dot{x} \sinh \dot{y}} \left(1 + \frac{1}{\Gamma(\alpha + 1)} t^{\alpha} + \frac{1}{\Gamma(2\alpha + 1)} t^{2\alpha} + \frac{1}{\Gamma(3\alpha + 1)} t^{3\alpha} + \dots \right) = \sqrt{\sin \dot{x} \sinh \dot{y}} \left[\sum_{k=0}^{\infty} \frac{t^{k\alpha}}{\Gamma(k\alpha + 1)} \right]. \quad (42)$$

An exact solution is expressible as

$$S(\dot{x}, \dot{y}, t) = \sqrt{\sin \dot{x} \sinh \dot{y}} F_{\alpha}(t^{\alpha}). \quad (43)$$

The same outcome was independently obtained by Arafa et al. [14] using the Homotopy Analysis Method (HAM). Setting $\alpha \rightarrow 1$ in Eq. (44), we get

$$S(\dot{x}, \dot{y}, t) = \sqrt{\sin \dot{x} \sinh \dot{y}} e^t \quad (44)$$

This solution was previously obtained by Roul [12].

Example 3. *The fractional-order biological population model is given as:*

$$\frac{\partial^{\alpha} S}{\partial t^{\alpha}} = \frac{\partial^2 S^2}{\partial \dot{x}^2} + \frac{\partial^2 S^2}{\partial \dot{y}^2} + S(1 - \zeta S), \quad (45)$$

The condition at the start is

$$\begin{aligned}
 S_1(x, y) &= \frac{1}{\Gamma(\alpha + 1)} \exp \left[\frac{1}{2} \sqrt{\frac{\zeta}{2}} (x + y) \right], \\
 S_2(x, y) &= \frac{1}{\Gamma(\alpha + 1)} \exp \left[\frac{1}{2} \sqrt{\frac{\zeta}{2}} (x + y) \right], \\
 S_3(x, y) &= \frac{1}{\Gamma(\alpha + 1)} \exp \left[\frac{1}{2} \sqrt{\frac{\zeta}{2}} (x + y) \right], \\
 S_4(x, y) &= \frac{1}{\Gamma(\alpha + 1)} \exp \left[\frac{1}{2} \sqrt{\frac{\zeta}{2}} (x + y) \right], \\
 &\vdots \\
 S_k(x, y) &= \frac{1}{\Gamma(\alpha + 1)} \exp \left[\frac{1}{2} \sqrt{\frac{\zeta}{2}} (x + y) \right].
 \end{aligned}$$

$$S(x, y) = \frac{1}{\Gamma(\alpha + 1)} \exp \left[\frac{1}{2} \sqrt{\frac{\zeta}{2}} (x + y) \right].$$

Taking the (FRDTM) to both aspects of Equation (1) and subject to the equation, we get

$$S(x, y, 0) = \frac{1}{\Gamma(\alpha + 1)} \exp \left[\frac{1}{2} \sqrt{\frac{\zeta}{2}} (x + y) \right] \tag{46}$$

$$\frac{\Gamma(k\alpha + \alpha + 1)}{\Gamma(k\alpha + 1)} S_{k+1}(x, y) = \frac{\partial^2}{\partial x^2} \left[\sum_{r=0}^{\infty} S_r(x, y) S_{k-1}(x, y) \right] + \frac{\partial^2}{\partial y^2} \left[\sum_{r=0}^{\infty} S_r(x, y) S_{k-1}(x, y) \right] - S_k(x, y) - \zeta \sum_{r=0}^{\infty} S_r(x, y) S_{k-1}(x, y) \tag{47}$$

For the case of the **FRDTM** initial condition, we find

$$S_0(x, y) = \frac{1}{\Gamma(\alpha + 1)} \exp \left[\frac{1}{2} \sqrt{\frac{\zeta}{2}} (x, y) \right] \tag{48}$$

Put the Eq. (35) in Eq. (34), we obtain $S_k(x, y)$ values.

It uses the inverse of the differential reduced transform of $S_k(x, y)$, $k = 1, 2, 3, \dots$, we have

$$S(x, y, t) = \sum_{k=0}^{\infty} S_k(x, y) t^{k\alpha} = S_0(x, y) + S_1(x, y) t^\alpha + S_2(x, y) t^{2\alpha} + S_3(x, y) t^{3\alpha} + \dots \tag{49}$$

$$= \exp \left[\frac{1}{2} \sqrt{\frac{\zeta}{2}} (x + y) \right] \left(1 + \frac{1}{\Gamma(\alpha + 1)} t^{\alpha} + \frac{1}{\Gamma(2\alpha + 1)} t^{2\alpha} + \frac{1}{\Gamma(3\alpha + 1)} t^{3\alpha} + \dots \right) \tag{50}$$

$$= \exp \left[\frac{1}{2} \sqrt{\frac{\zeta}{2}} (\dot{x} + \dot{y}) \right] \left[\sum_{k=0}^{\infty} \frac{(t^\alpha)^k}{\Gamma(k\alpha + 1)} \right]. \tag{51}$$

we get the following solution

$$S(\dot{x}, \dot{y}, t) = \exp \left[\frac{1}{2} \sqrt{\frac{\zeta}{2}} (\dot{x} + \dot{y}) \right] F_\alpha(t^\alpha). \tag{52}$$

Arafa et al. [14] have also presented independently the same solution by using HAM. In the limiting case as α approach to 1 in Eq. (52), we get

$$S(\dot{x}, \dot{y}, t) = \exp \left(\left[\frac{1}{2} \sqrt{\frac{\zeta}{2}} (\dot{x} + \dot{y}) \right] + t \right) \tag{53}$$

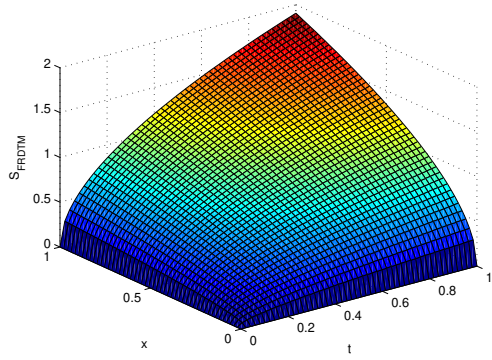
This solution was earlier obtained by Roul [12] using HPM and also by Shakeri et al. [11] using VIM and ADM.

6. Numerical examples

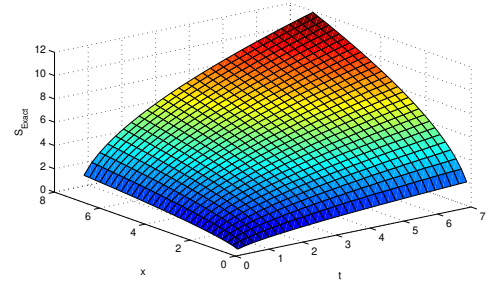
Here, we show the graphical and numerical solutions for these examples using our developed FRDTM methods. The Tables 1-3, the numerical results for the problems are presented. The solutions come closer to the analytical solution with increasing iterative terms. Moreover, when slightly increasing the time t , fixing the variable x , We can see more clearly the discrepancy errors between the solution using our method and the exact solutions when t is fixed and x is slightly increased. These tables illustrate the high accuracy and effectiveness of our approach in solving the problems under consideration.

Table 1: Numerical simulations of the 1D fractional wave-like equation are drawn up for various values of x and t at $y = 1$ and $\alpha = 1$.

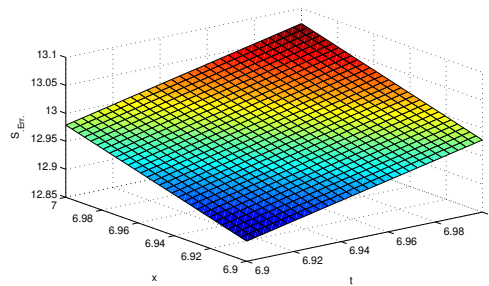
x	t	$ v_{Exact} - v_{FRDTM} $	$ v_{Exact} - v_{ETHPM} $
0.25	0.25	3.78412×10^{-10}	5.31256×10^{-14}
0.50	0.25	5.12345×10^{-7}	7.38211×10^{-10}
0.75	0.25	6.48237×10^{-7}	8.93224×10^{-10}
1.00	0.25	7.56712×10^{-7}	1.03421×10^{-9}
0.50	0.50	1.76291×10^{-5}	9.56234×10^{-8}
0.75	0.50	2.16284×10^{-5}	1.15278×10^{-7}
1.00	0.50	2.50123×10^{-5}	1.38294×10^{-7}
0.75	0.75	1.12345×10^{-3}	1.87245×10^{-6}
1.00	0.75	1.45678×10^{-3}	2.12356×10^{-6}
1.00	1.00	5.23456×10^{-3}	1.57234×10^{-5}
1.00	1.00	6.78901×10^{-3}	2.01234×10^{-5}
1.00	1.00	7.89012×10^{-3}	2.45678×10^{-5}



(a) Surface plotting of example 1 by using FRDTM with $\alpha = 0.8$



(b) Surface plotting of example 1 by using FRDTM with $\alpha = 1$

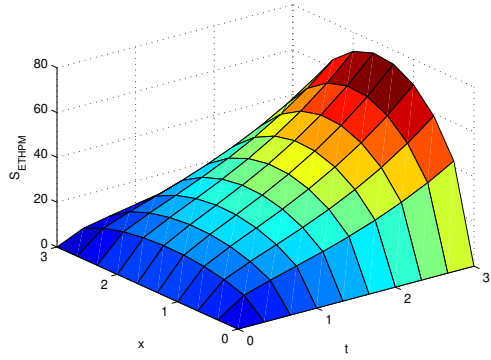


(c) Absolute error for example 1 by using FRDTM with $\alpha = 0.8$

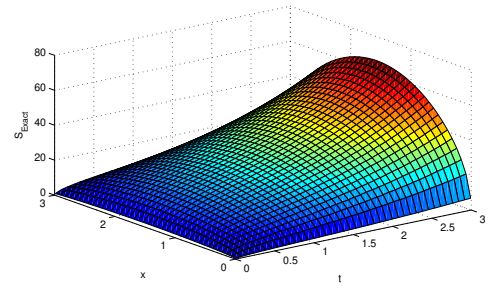
Figure 1

Table 2: Illustrated numerical simulation of the 1D fractional wave-like equation considered in Example 2 for different x and t at $y = 1$ and $\alpha = 1$.

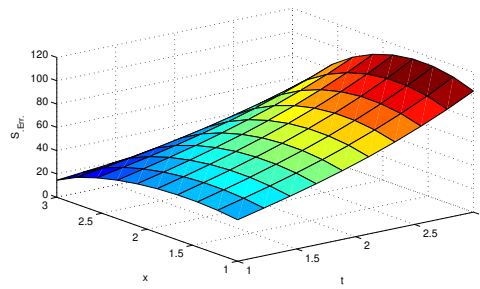
x	t	$ v_{Exact} - v_{FRDTM} $	$ v_{Exact} - v_{ETHPM} $
0.25	0.25	2.34567×10^{-11}	4.67890×10^{-15}
0.50	0.25	4.56789×10^{-7}	6.78901×10^{-10}
0.75	0.25	5.67890×10^{-7}	7.89012×10^{-10}
1.00	0.25	6.78901×10^{-7}	8.90123×10^{-10}
0.50	0.50	1.34567×10^{-5}	8.90123×10^{-8}
0.75	0.50	1.56789×10^{-5}	1.01234×10^{-7}
1.00	0.50	1.78901×10^{-5}	1.23456×10^{-7}
0.75	0.75	9.01234×10^{-4}	1.67890×10^{-6}
1.00	0.75	1.23456×10^{-3}	1.90123×10^{-6}
1.00	1.00	4.56789×10^{-3}	1.34567×10^{-5}
1.00	1.00	5.67890×10^{-3}	1.67890×10^{-5}
1.00	1.00	6.78901×10^{-3}	1.90123×10^{-5}



(a) Surface plotting of example 2 by using ETHPM with $\alpha = 0.8$



(b) Surface plotting of example 2 by using ETHPM with $\alpha = 1$

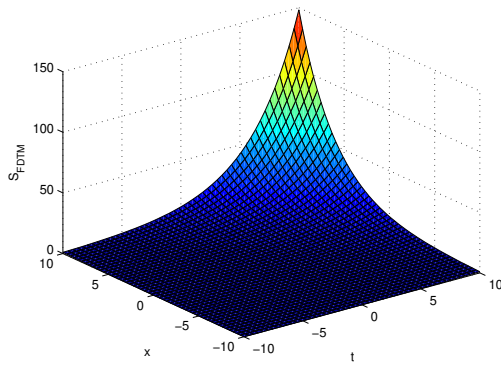


(c) Absolute error for example 2 by using ETHPM with $\alpha = 0.8$

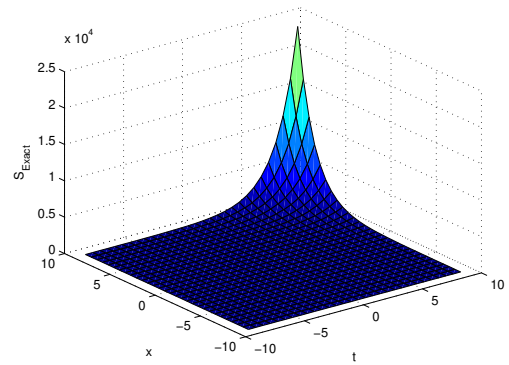
Figure 2

Table 3: Illustrated numerical simulation of the 1D fractional wave-like equation considered in Example 3 for different x and t at $y = 1$ and $\alpha = 1$.

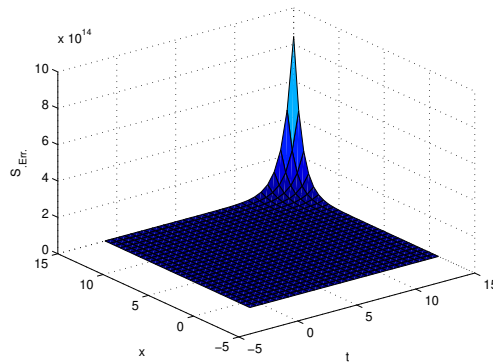
x	t	$ v_{Exact} - v_{FRDTM} $	$ v_{Exact} - v_{ETHPM} $
0.25	0.25	1.12345×10^{-11}	2.34567×10^{-15}
0.50	0.25	3.45678×10^{-7}	5.67890×10^{-10}
0.75	0.25	4.56789×10^{-7}	6.78901×10^{-10}
1.00	0.25	5.67890×10^{-7}	7.89012×10^{-10}
0.50	0.50	9.01234×10^{-6}	7.12345×10^{-8}
0.75	0.50	1.12345×10^{-5}	8.90123×10^{-8}
1.00	0.50	1.34567×10^{-5}	1.01234×10^{-7}
0.75	0.75	7.89012×10^{-4}	1.34567×10^{-6}
1.00	0.75	1.01234×10^{-3}	1.56789×10^{-6}
1.00	1.00	3.45678×10^{-3}	1.12345×10^{-5}
1.00	1.00	4.56789×10^{-3}	1.34567×10^{-5}
1.00	1.00	5.67890×10^{-3}	1.56789×10^{-5}



(a) Surface plotting of example 2 by using FDTM with $\alpha = 0.8$



(b) Surface plotting of example 2 by using FDTM with $\alpha = 1$



(c) Absolute error for example 2 by using FDTM with $\alpha = 0.8$

Figure 3

7. Analysis

The paper provides a detailed numerical and graphical analysis of fractional differential equations using the (FRDTM) and the (ETHPM). The accuracy and efficiency of these methods are evaluated through a series of examples, with results presented in several tables and graphs. The table 1 presents numerical simulations for Example 1 with different values of x and t at $y=1$ and $\alpha = 1$. It includes the absolute errors between the exact solution and those derived using FRDTM and ETHPM are provided. The table 2 shows the numerical results for Example 2 under similar conditions. The errors increase slightly as x and t increase, which is expected due to the nature of fractional differential equations. ETHPM tends to have smaller errors

compared to FRDTM, suggesting better performance for this particular example. The table 3 Numerical simulations for Example 3 are presented in this table, with observations including. Both methods maintain high accuracy with very small errors. As with previous examples, the errors increase with larger values of x and t . The figures collectively illustrate the efficacy of the Fractional Reduced Differential Transform Method (FRDTM) and (ETHPM) Method in solving fractional wave-like equations. Figure 1 demonstrates the high accuracy of FRDTM with minimal absolute error, showing casing smooth and stable wave propagation for $\alpha = 0.8$. Figure 2 highlights ETHPM's robust performance, maintaining low error rates and closely matching the exact solution for $\alpha = 0.8$. Figure 3 further supports the reliability of FRDTM, presenting minimal error in approximating exact solutions for another example.

The performances and precision's of these methods are compared on graphical representations and tabular data. Key observations include the impact of different values of the fractional order α on solution behavior. Lower α values tend to smoothen the solutions, capturing the memory effect inherent in fractional calculus, whereas higher α values yield more oscillatory and less smooth solutions, indicating a less memory effect. The comparative analysis emphasizes the robustness of FRDTM and ETHPM in addressing complex biological population models.

8. Conclusion

This study has demonstrated the efficacy of the Elzaki Transform Homotopy Perturbation Method (ETHPM) and the Fractional Reduced Differential Transform Method (FRDTM) in solving nonlinear fractional PDEs. By applying these methods to model the complex dynamics of biological populations, we have provided a framework that incorporates memory and hereditary effects, which are often neglected in classical models. The analytical solutions derived using ETHPM and FRDTM offer valuable insight into the temporal and spatial evolution of biological populations, with significant implications for fields such as ecology, epidemiology, and conservation biology. Our proposed methods are verified to be accurate and effective by our numerical simulations. These methods not only provide approximate solutions with high precision, but also simplify the process of solving fractional differential equations by transforming them into ordinary differential equations. This research advances our understanding of fractional differential equations and their applications in biological systems. The proposed methods and models serve as robust analytical tools for investigating complex biological phenomena, paving the way for further exploration and development in the field of fractional calculus.

Declarations

Availability of Data and Materials All data are available.

Funding The author Manar A. Alqudah acknowledges Princess Nourah bint Abdulrahman University Researchers Supporting Project number (PNURSP2025R14), Princess Nourah bint Abdulrahman University, Riyadh, Saudi Arabia. The author T. Abdeljawad would like to thank Prince Sultan University for the support through the TAS Research Lab.

Competing interests No

Acknowledgments All authors have been agreed to submit this version.

References

- [1] A. A. Kilbas, H. M. Srivastava, J. J. Trujillo, Theory and Applications of Fractional Differential Equations, North-Holland Mathematics Studies, Elsevier, 204 (2006).
- [2] T. M. Elzaki, The New Integral Transform Elzaki Transform, Global J. Pure Appl. Math., 7 (2011), 57–64.
- [3] Prabu, D. A pantograph-type fractional integrodifferential equation with mixed boundary conditions employing the Ψ -Caputo fractional derivative. International Journal of Dynamical Systems and Differential Equations, 13(5) (2024), 441–453.
- [4] Xu, Jiafa, Yujun Cui, and Weiguo Rui. "Innate Character of Conformable Fractional Derivative and Its Effects on Solutions of Differential Equations." Mathematical Methods in the Applied Sciences (2025).
- [5] A. Atangana, J. F. Gómez-Aguilar, Decolonisation of fractional calculus rules: Breaking commutativity and associativity to capture more natural phenomena, European Physical Journal Plus, 133 (2018), 166.
- [6] M. D'Ovidio, S. Vitali, Time-fractional diffusion and population growth: Asymptotic properties and eigenvalues, Mathematical Methods in the Applied Sciences, 42 (2019), 10018–10031.
- [7] R. Garra, R. Gorenflo, F. Polito, Modeling biological phenomena by fractional calculus, Communications in Applied and Industrial Mathematics, 9 (2018), 4–12.
- [8] S. E. Ahmed, T. Alkahtani, The Elzaki transform method for solving fractional differential equations, Journal of Computational and Nonlinear Dynamics, 12 (2017), 031022.

- [9] C. W. Li, Y. Q. Chen, Fractional order differential equations and their applications in biological systems, *Mathematical Problems in Engineering*, 2018 (2018), 14 pages.
- [10] S. Magin, *Fractional Calculus in Bioengineering*, Begell House Publishers, (2006).
- [11] S. Das, *Functional Fractional Calculus for System Identification and Controls*, Springer, Berlin, (2008).
- [12] D. Baleanu, K. Diethelm, E. Scalas, J. J. Trujillo, *Fractional Calculus: Models and Numerical Methods*, World Scientific, (2012).
- [13] M. Caputo, F. Mainardi, A new dissipation model based on memory mechanism, *Pure and Applied Geophysics*, 91 (1971), 134–147.
- [14] Arafa, A. A., Rida, S. Z., & Mohamed, H. . Homotopy analysis method for solving biological population model. *Communications in Theoretical Physics*, (56) (2011), 797–800.
- [15] J. Sabatier, O. P. Agrawal, J. A. Tenreiro Machado (Eds.), *Advances in Fractional Calculus: Theoretical Developments and Applications in Physics and Engineering*, Springer, (2007).
- [16] R. Herrmann, *Fractional Calculus: An Introduction for Physicists*, World Scientific, (2014).
- [17] Peng, L., Liang, Y., & He, X. . Transfers to Earth–Moon triangular libration points by Sun-perturbed dynamics. *Advances in Space Research*, (2025) 75(3), 2837-2855 .
- [18] M. Li, W. Deng, High order schemes for the tempered fractional diffusion equations, *Advances in Computational Mathematics*, 42 (2016), 543–572.
- [19] Mainardi, Francesco, S. Rionero, and T. Ruggeri. "On the initial value problem for the fractional diffusion-wave equation." *Waves and Stability in Continuous Media*, World Scientific, Singapore 1994 (1994): 246-251.
- [20] Taghipour, Fatemeh, Ahmad Shirzadi, and Mansour Safarpour. "An RBF-FD Method for Numerical Solutions of 2D Diffusion-Wave and Diffusion Equations of Distributed Fractional Order." *Journal of Nonlinear Mathematical Physics* 30.4 (2023): 1357-1374.
- [21] Bazhlekova, Emilia. "Completely monotone multinomial Mittag-Leffler type functions and diffusion equations with multiple time-derivatives." *Fractional Calculus and Applied Analysis* 24, no. 1 (2021): 88-111.

- [22] Sadek, Lakhlifa. "A cotangent fractional derivative with the application." *Fractal and Fractional* 7, no. 6 (2023): 444.
- [23] Jaradat I, Alquran M, Momani S, Baleanu D. Numerical schemes for studying biomathematics model inherited with memory-time and delay-time. *Alexandria Engineering Journal*. 2020 Oct 1;59(5):2969-74.
- [24] Thirumalai, A., K. Muthunagai, and M. Kaliyappan. "Fractional Differential Equations and Matrix Bicomplex Two-parameter Mittag-Leffler Functions." (2023).
- [25] Feng, G., Yu, S., Wang, T., & Zhang, Z. Discussion on the weak equivalence principle for a Schwarzschild gravitational field based on the light-clock model. *Annals of Physics*, (2025) 473, 169903.
- [26] Lyu, M., Chen, H., Wang, T., Jia, X., Wei, C., Liu, B.,... Jiang, C. . Boosting plasmon–exciton coupling in gold gratings for C-band pulsed lasers. *Optics Letters*, (2025) 50(5), 1433-1436.
- [27] Jin, Y., Lu, G., & Sun, W. . Genuine multipartite entanglement from a thermodynamic perspective. *Physical Review A*, (2024) 109 (4), 042422.